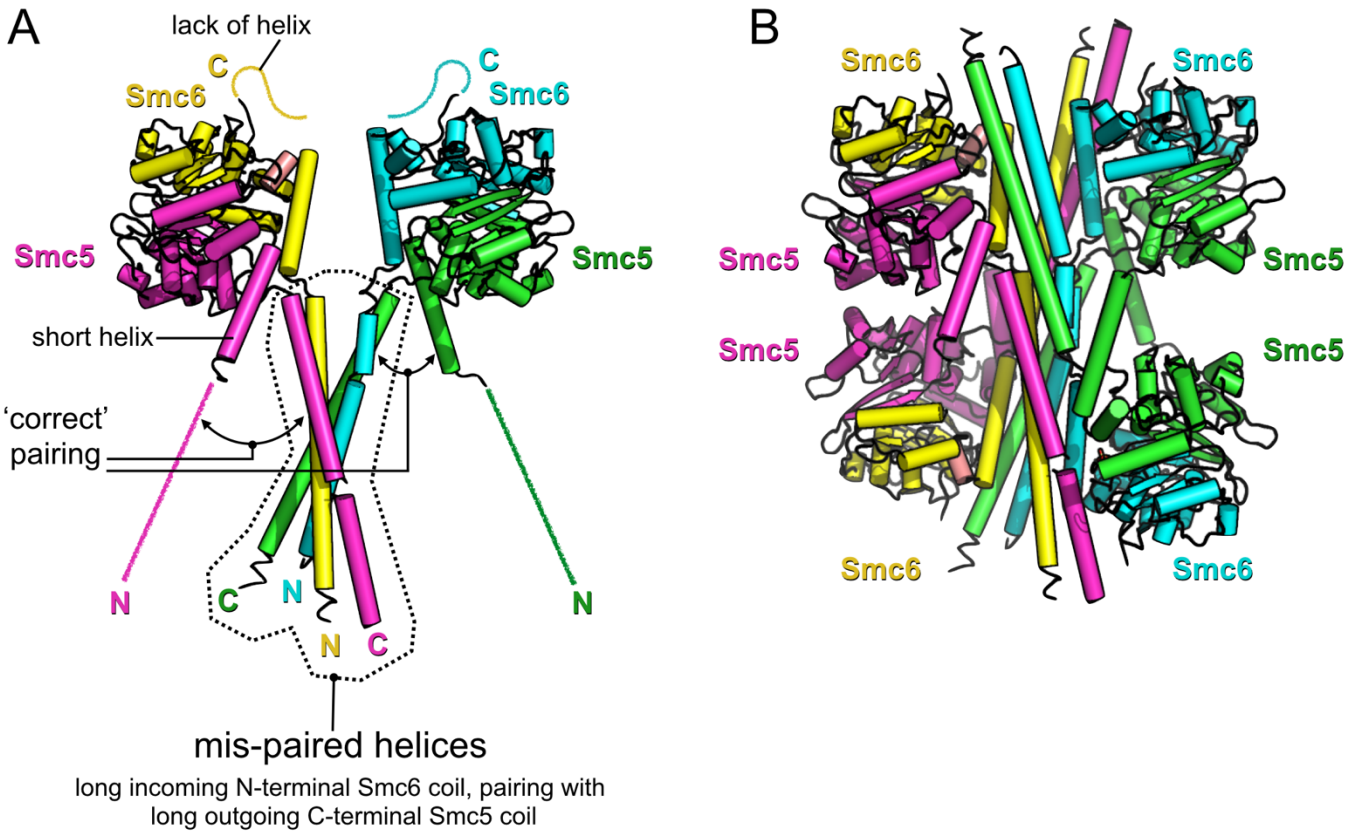


C

**Smc5**

```
                310       320       330       340       350       360
ASMELNTSNL RARASFSNFM ENEKKLYEKV NTNRTLLRNA NLTLNEAQQS VKSLTERQGP

364↓            370       380       390       400       410       420
RPSDNGVQDL QEKMQEVNAE KLQHENEKLE SSHELGSIRT LKAQKLIDLD NIKRELSYYN
                                                  408↑ coiled-coil
                430       440       450       460       470       480
DATKRKLDFM SSAPGWEDAY QTYQLLKEYE SAFEAPAYGP IYMNLKCKEK GFAALIEGFF
                      *   α1        α2        α3    β1  α4
                490       500       510       520       530       540
RTDTFRTFIM SNYNDYLKLM DLITSKTKYT PTIREFSSER KKKIEDFEPP CSREKLQSFG
            β2    α5        α5        β3        α6        α7
                550       560       570       580       590       600
FDGYVIDFLE GPEVVLVALC HMLKIHQIPI AKRELPPASV NALNNFRLAN GDPVLKTYLA
            β4 α8 β5  α9        β6        α10       *         β7
                610       620       630       640       650       660
GSSIHLVFRS AYGDREITRR TDPLPSRSIY FSENVEMDLV KRKEEQLNAQ LSQLENLQNE
            β8    ** * * β9                                   658↑
                670       680       690       700       710       720
ERKLQEKVNE HESLLSRTND ILSTLRKERD EKLIPIHEWQ QLQERIEHQT LLLRQREKVP
coiled-coil                                   692↑
```

**Smc6**

```
                430       440       450       460       470       480
SINAAKSCLD VYREQLNTER ARENNLGGSQ IEKRANESNN LQREIADLSE QIVELESKRN
                                          462↓ coiled-coil
                490       500       501↓      520       530       540
DLHSALLEMG GNLTSLLTKK DSIANKISDQ SEHLKVLEDV QRDKVSAFGK NMPQLLKLIT
                      α1        α2        α3 *      α4
                550       560       570       580       590       600
RETRFQHPPK *GPMGKYMTVK EQKWHLIIER ILGNVINGFI VRSHHDQLIL KELMRQSNCH
                α5    β1  α6        α7    β2  α8
                610       620       630       640       650       660
ATVVVGKYDP FDYSSGEPDS QYPTVLKIIK FDDDEVLHTL INHLGIEKML LIEDRREAEA
            β3    α10       α11   β4  α12       α13   β5  α14
                670       680       690       700       710       720
YMKRGIANVT QCYALDPRNR GYGFRIVSTQ RSSGISKVTP WNRPPRIGFS SSTSIEAEKK
                β6        β7        β8        β9
                730       740       750       760       770       780
ILDDLKKQYN FASNQLNEAK IEQAKFKRDE QLLVEKIEGI KKRILLKRRE VNSLESQELS
                      737↑                            773↑
```

coiled-coil 'arm'
α-helix
β-strand

LSQL crystal
↑ extended-hinge
↑ truncated-hinge
*Y mutant in this study

**Supplementary Figure 1**

**The asymmetric unit of Smc5/6-hinge crystals**

(A) The asymmetric unit of Smc5/6-hinge crystals contains two hetero-dimers, shown in molecular cartoon representation. Smc5 is coloured magenta and green, and Smc6 yellow and cyan. The constructs expressing Smc5 (aa 336-692) and Smc6 (448-703) encode mismatched lengths of coiled-coil, at both the N- and C-termini. This has resulting in mis-pairing of the incoming N-terminal coil of Smc6, with the outgoing C-terminal coil of Smc5 in the asymmetric unit. (B) Partially expanded crystal lattice, highlighting the complex arrangement of the component hetero-dimers. (C) Annotated amino acid sequence for the hinge-regions of *S.pombe* Smc5 and Smc6. See associated key for full details.

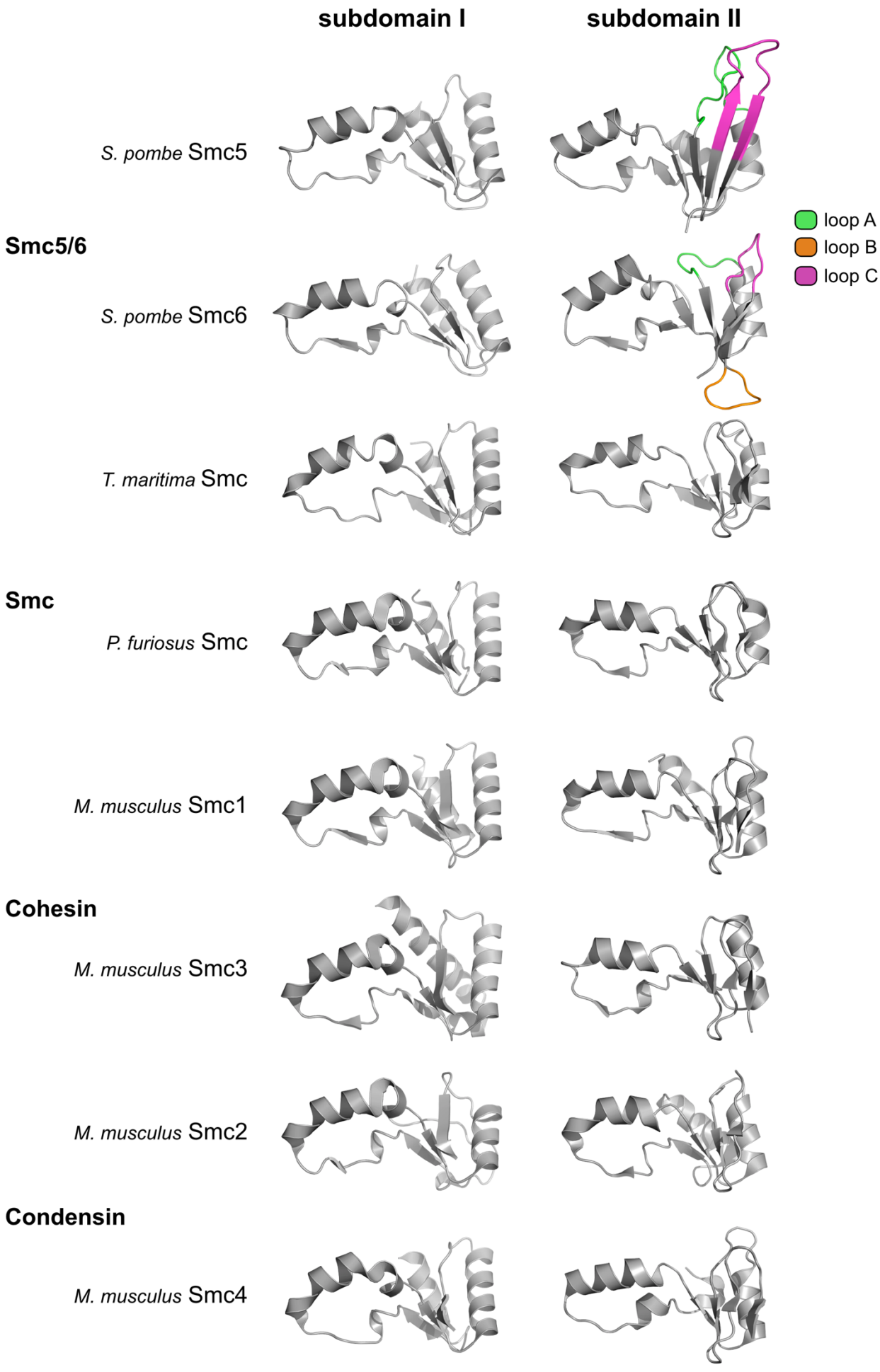
subdomain I
subdomain II
S. pombe Smc5
Smc5/6
S. pombe Smc6
T. maritima Smc
Smc
P. furiosus Smc
M. musculus Smc1
Cohesin
M. musculus Smc3
M. musculus Smc2
Condensin
M. musculus Smc4
loop A
loop B
loop C

**Supplementary Figure 2**

**Subdomains of selected SMC-family proteins**

Molecular cartoon representations are show for subdomain I (left) and subdomain II (right) for the indicated SMC proteins. The points of amino acid insertion in subdomain II of Smc5 and Smc6 are additionally highlighted. Loop A, B and C are coloured green, orange and magenta respectively.

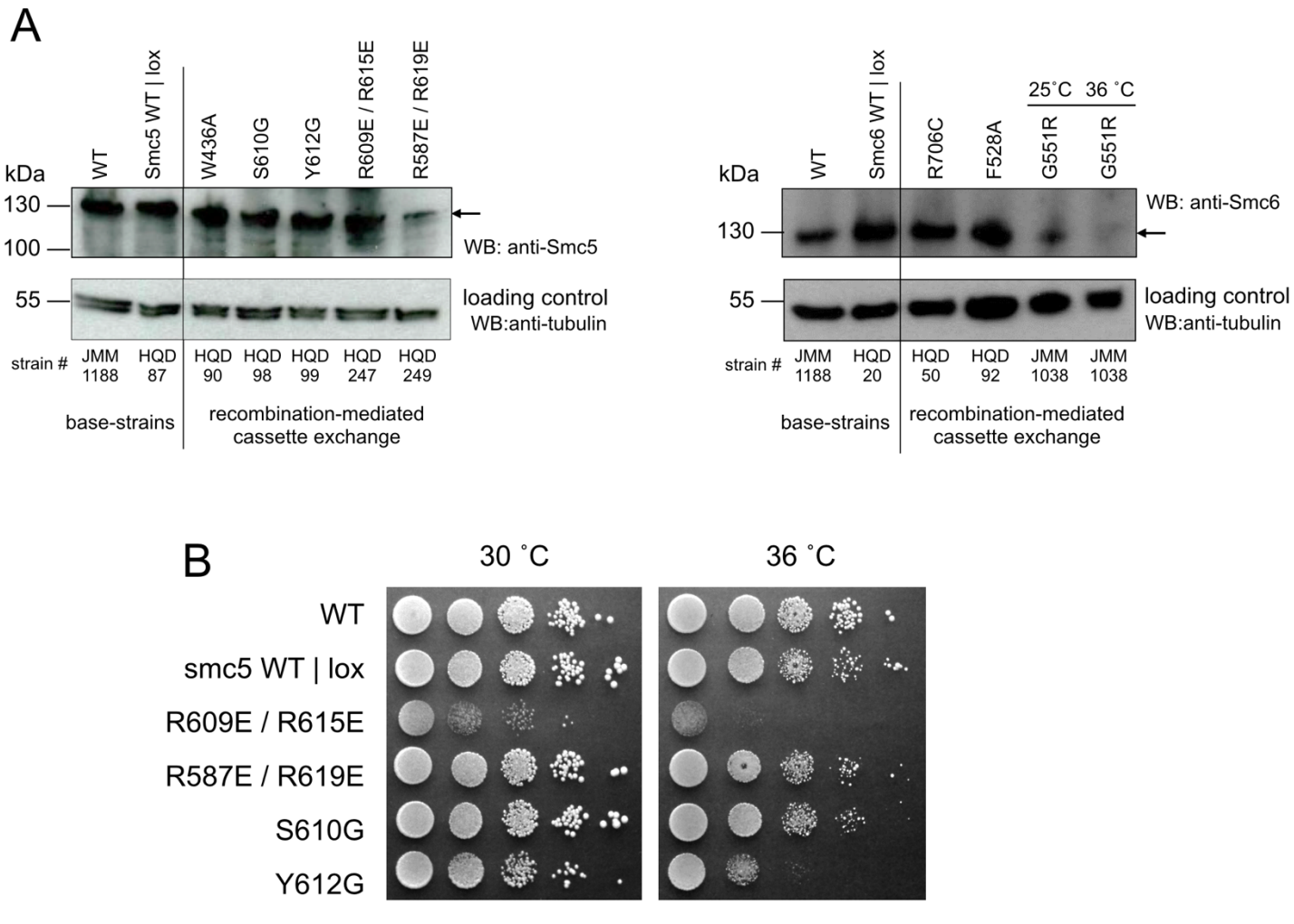


**Supplementary Figure 3**

**Analysis of yeast strains**

(A, left) Western blot confirming expression of Smc5 in the indicated *S.pombe* strains. (A, right) Western blot confirming expression of Smc6 in the indicated *S.pombe* strains. The JMM1038 strain, containing the temperature sensitive Smc6 mutation G551R (*smc6-T2*) was incubated at 25 °C or 36 °C for a period of 4 hours prior to harvesting and lysis. The loss of signal at 36 °C confirms specificity of the Smc6 antibody. (B) Temperature sensitivity of Smc5-Loop C and Arginine-pair mutants.

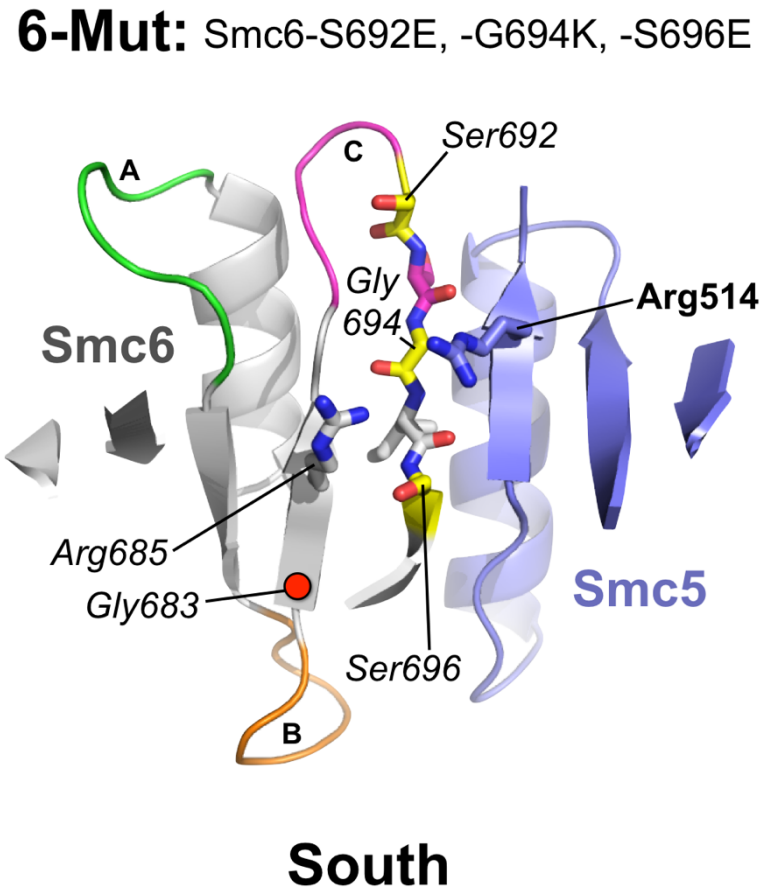


**Supplementary Figure 4**

**Molecular details for the 6-Mut series of mutations**

Molecular cartoon representation of the 'South' interface, highlighting the position of the amino acids mutated in Smc6, in order to generate '6-Mut' (coloured in yellow).

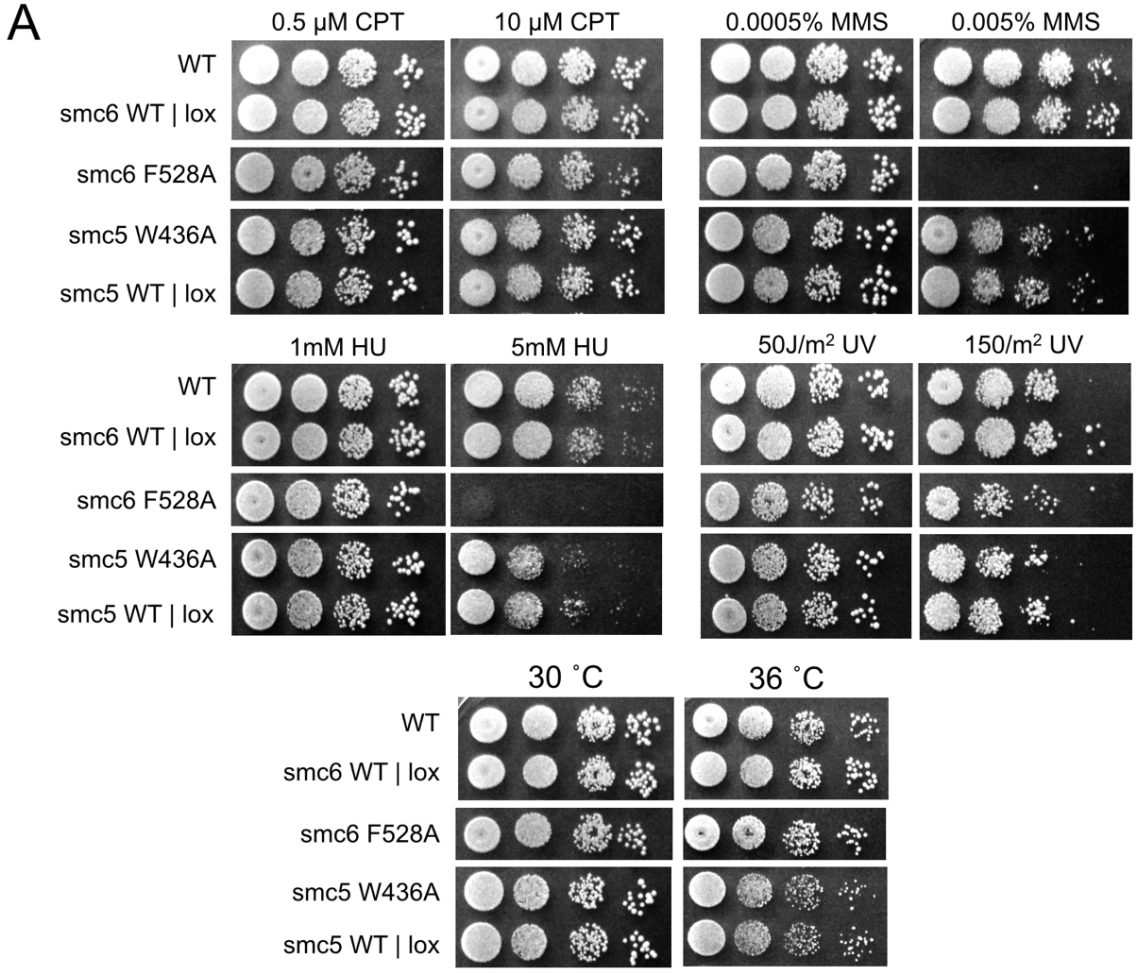
A
0.5 µM CPT
10 µM CPT
0.0005% MMS
0.005% MMS
WT
smc6 WT | lox
smc6 F528A
smc5 W436A
smc5 WT | lox
1mM HU
5mM HU
50J/m2 UV
150/m2 UV
30 ˚C
36 ˚C

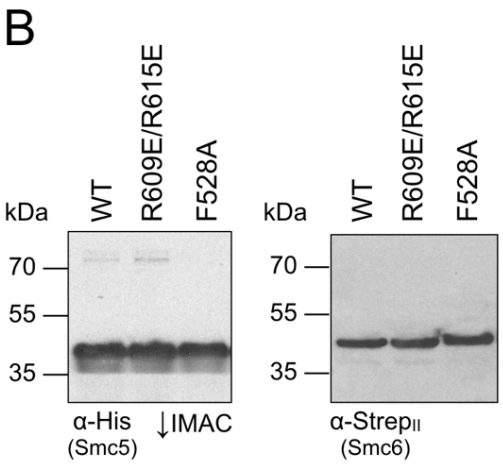
B
kDa
WT
R609E/R615E
F528A
70
55
35
α-His
(Smc5)
↓IMAC
α-Strep II
(Smc6)

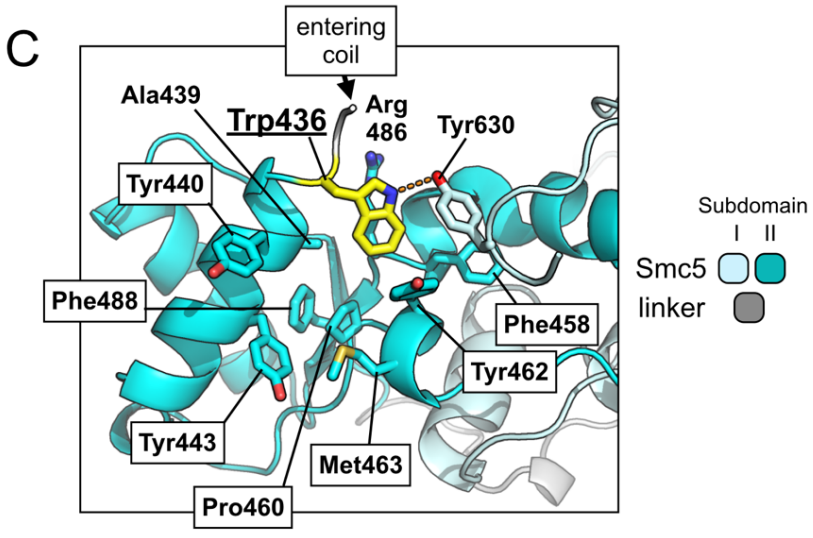
C
entering coil
Ala439
Trp436
Arg 486
Tyr630
Tyr440
Phe488
Phe458
Tyr462
Tyr443
Met463
Pro460
Subdomain
I II
Smc5
linker

**Supplementary Figure 5**

**DNA damage and temperature sensitivity of the Smc6-F528A and Smc5-W436A *S.pombe* strains**

(A) Doses and type of treatment are as indicated. (B) Co-expression / co-purification assay. His-Tagged Smc5-hinge was co-expressed with StrepII-tagged Smc6-hinge in *E.coli.* After lysis, and clarification, the soluble fraction was passed through a IMAC column, capturing Smc5-hinge. After successive washes, to remove any unbound material, the amount of co-purified Smc6-hinge was assessed by western blot. (C) Molecular details of the Smc5-W436 locus – which is predominantly hydrophobic in nature. Key amino acids residues are labelled. Trp436 is additionally highlighted in yellow.

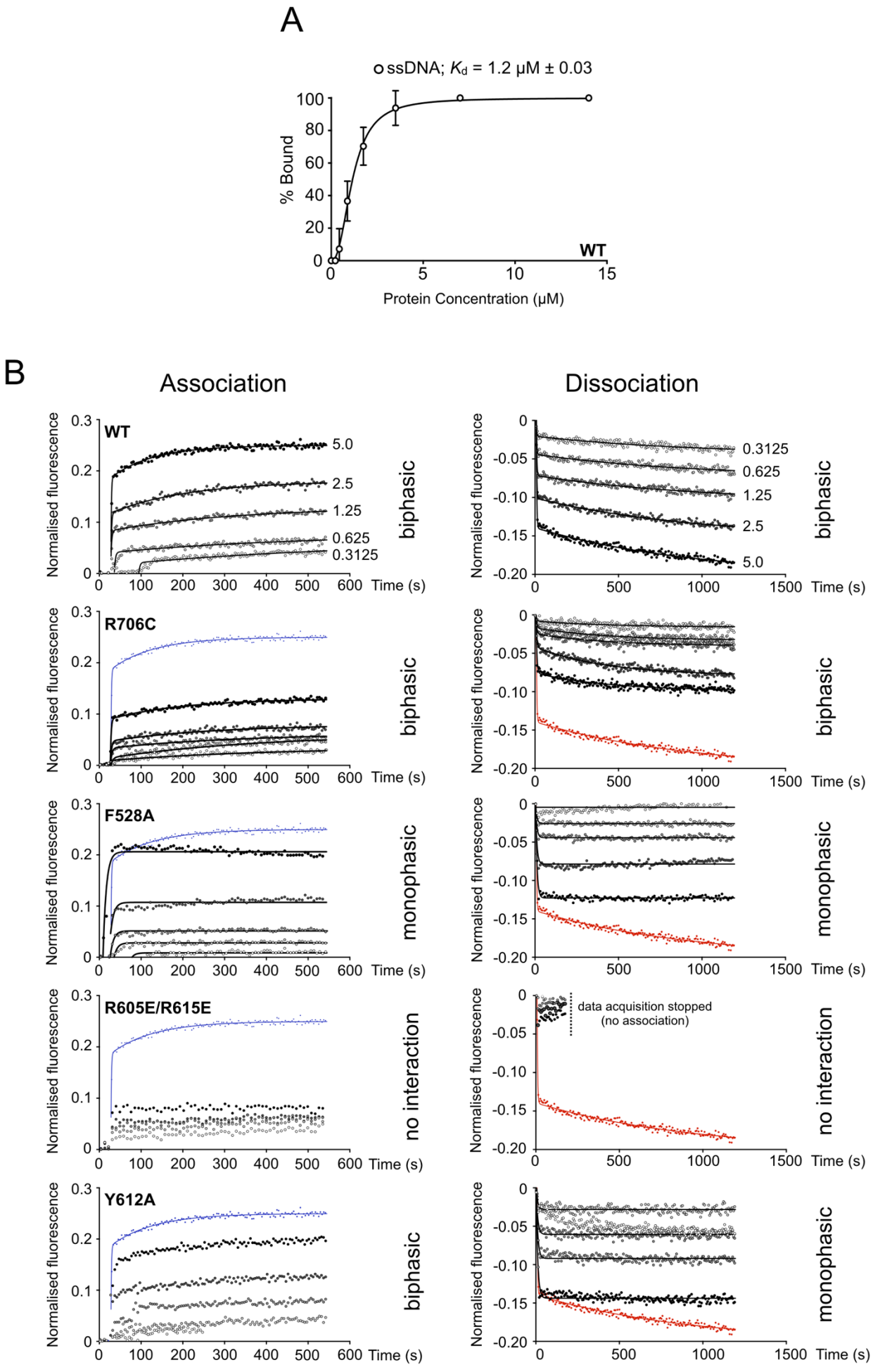
A
ssDNA; $K_d$ = 1.2 µM ± 0.03
% Bound
Protein Concentration (µM)
WT
B
Association
Dissociation
Normalised fluorescence
Time (s)
WT
5.0
2.5
1.25
0.625
0.3125
biphasic
R706C
biphasic
F528A
monophasic
R605E/R615E
no interaction
data acquisition stopped
(no association)
Y612A
biphasic
0.3125
0.625
1.25
2.5
5.0
biphasic
biphasic
monophasic
no interaction
monophasic

**Supplementary Figure 6**

**Interactions of WT and mutant Smc5/6-hinge with ssDNA**

(A) Quantification of EMSA experiment (Figure 6B in manuscript), data-points represent the mean of 3 experiments, with error bars indicating one standard deviation. Dissociation constants ($K_d$) were determined by least-squares fitting of a one-site model. (B) Representative SwitchSENSE association and dissociation $F_{down}$ sensorgrams for the indicated Smc5/6-hinge protein. For ease of comparison the association (coloured blue) or dissociation curve (red) for the wild-type protein at a concentration of 5 μM is also shown for each mutant.

A

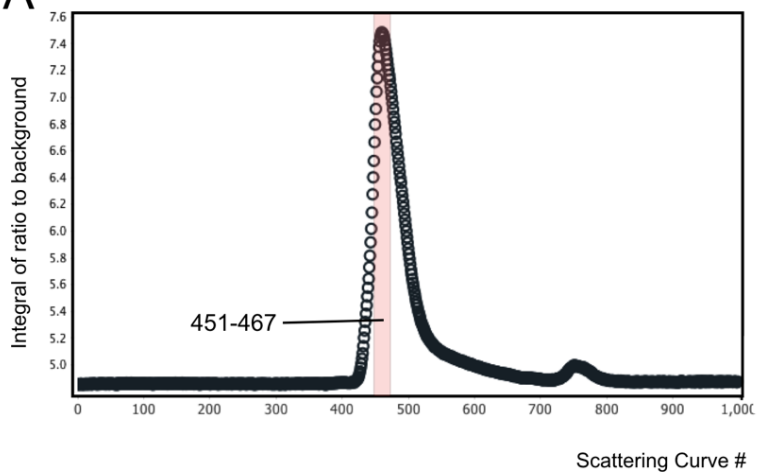


B

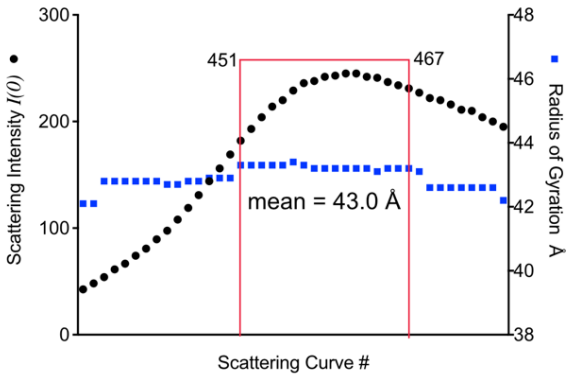


C

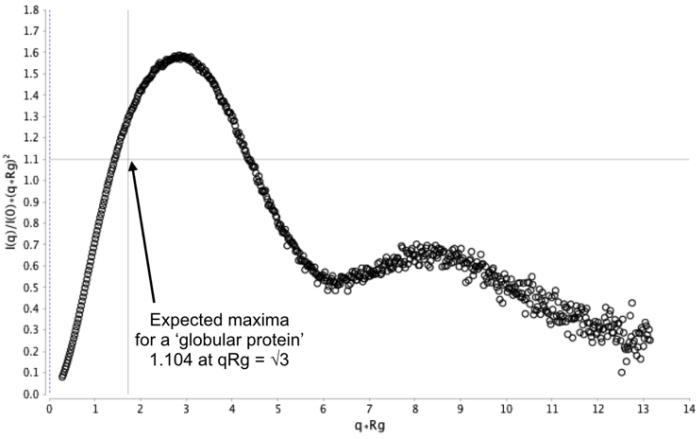


D

| | **ATSAS** (2.7.2) | **ScÅtter** (3.0c) |
|---|---|---|
| Guinier $R_g$, Å | 44.6 ± 1.5 | 43.0 |
| Guinier I(0), arbitrary units | 234.6 ± 0.3 | 231 |
| Quality | 0.96 | - |
| Aggregated? | 0.0049 | - |
| P*(r)* $R_g$, Å | 45.1 ± 0.4 | 44.7 |
| P*(r)* I(0), arbitrary units | 235 ± 0.9 | 232 |
| Porod volume estimate, Å$^3$ | 161185 | 178207 |
| $D_{max}$, Å | 156 | 165 |

**Supplementary Figure 7**

**Supporting data for Small-angle X-ray Scattering (SAXS) experiments**

(A,B) Scattering profiles corresponding to curves #451-467 (red rectangle) were selected for downstream analysis and averaging; they covered a wide concentration range, yet produced a consistent value for $R_g$ of ~43 Å (ScÅtter[1])

(C) Dimensionless Kratky plot (ScÅtter) for the scattering profile, obtained by merging and averaging curves #451-467. The Smc5/6-hinge does not have a compact, globular structure in solution, it instead adopts an extended conformation with some intrinsic level of flexibility[2].

(D) Summary of parameters determined for Smc5/6-hinge using SAXS with the indicated software packages ATSAS[3] and ScÅtter[1].

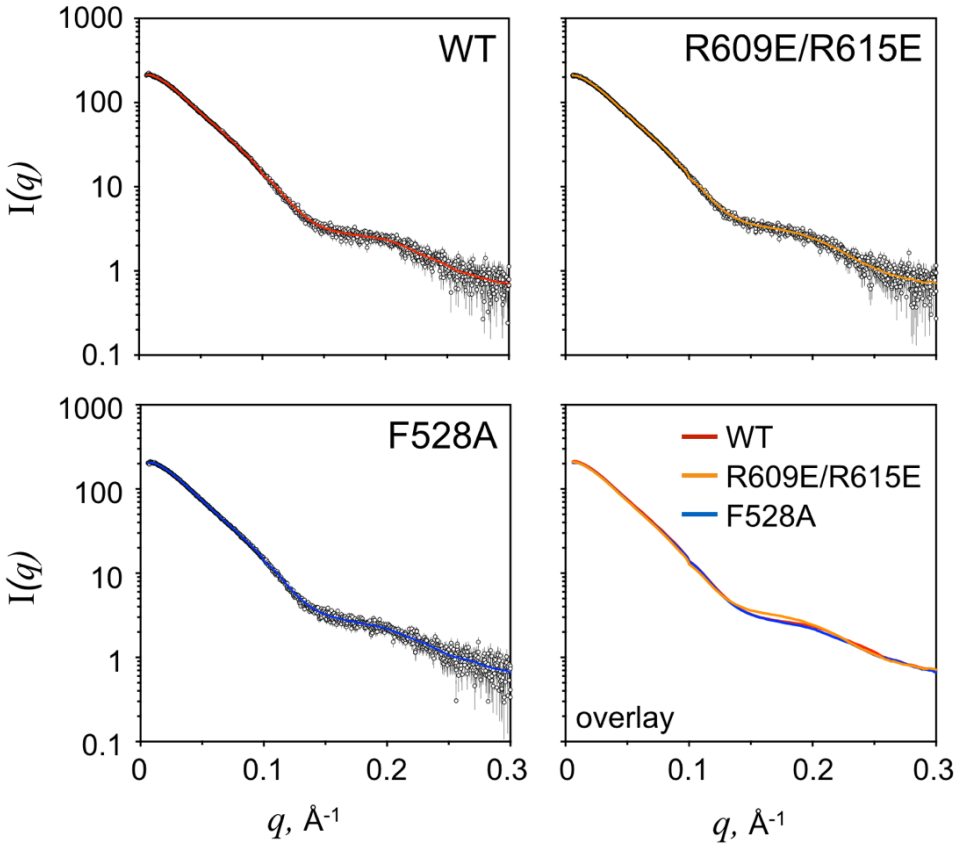


**Supplementary Figure 8**

**Scattering profiles of WT Smc5/6-hinge, R609E/R615E and F528A mutants**

Experimental data (open circles) with smoothed polynomial line-of-best-fit are shown in each case.

**Figure 3B** [ reverse orientation ]

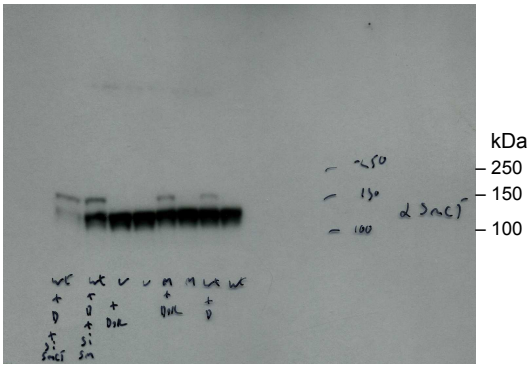


α-Smc5

**Figure 3B** [ reverse orientation ]

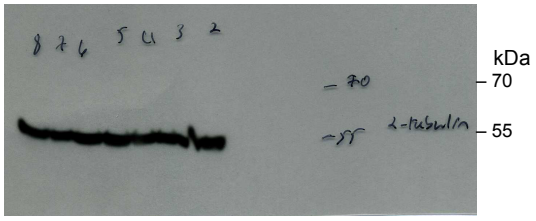


α-tubulin

**Figure 4D** α-Strep$_{II}$ (Smc6)

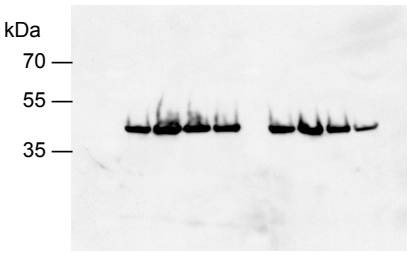


**Figure 4D** α-His (Smc5)

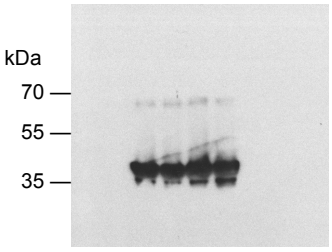


**Figure 4D** α-Strep$_{II}$ (Smc6)

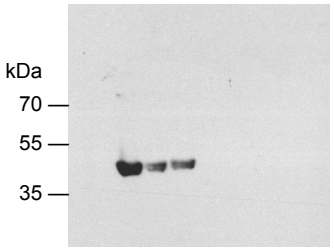


**Figure 6B**

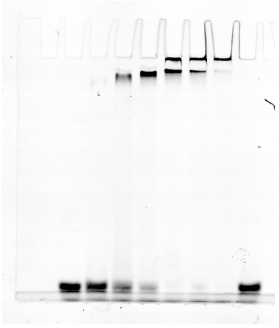

**Figure 6B inset**

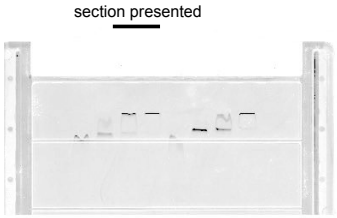


**Figure 6B inset**

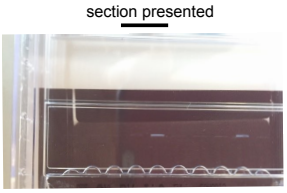


**Figure 6C**

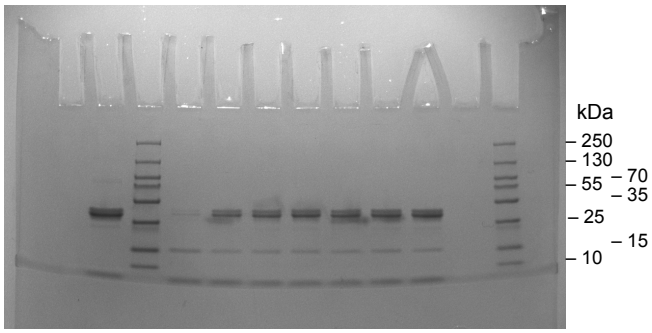


## Supplementary Figure 9

## Uncropped / uncapped images of gels and western blots

**Supplementary Table 1**

**Amino acid boundaries of expression constructs**

| | Smc5 | | Smc6 | |
|---|---|---|---|---|
| | N-terminus | C-terminus | N-terminus | C-terminus |
| Crystal structure | 336 | 692 | 448 | 703 |
| Extended-hinge | 364 | 692 | 462 | 773 |
| Truncated-hinge | 408 | 658 | 501 | 737 |

**Supplementary Table 2**

**X-ray diffraction: Data collection, phasing and refinement statistics**

| | Native | SeMet |
|---|---|---|
| **Data collection** | | |
| Space group | $C222_1$ | $C222_1$ |
| Cell dimensions | | |
| *a*, *b*, *c* (Å) | 172.56 196.46 122.44 | 171.36, 195.06, 121.18 |
| $\alpha, \beta, \gamma$ (°) | 90, 90, 90 | 90, 90, 90 |
| Wavelength | 0.9795 | 0.9788 |
| Resolution (Å) | 45.6 (2.75) | 48.8 (4.7) |
| *Mn I* / $\sigma I$ | 11.9 (1.4) | 11.4 (8.9) |
| *Mn I*, $CC_{1/2}$ | 0.998 (0.530) | 0.995 (0.983) |
| Completeness (%) | 100 (100) | 99.9 (100) |
| Redundancy | 6.6 (6.7) | 12.6 (12.9) |
| **Refinement** | | |
| Resolution (Å) | 45.6 (2.75) | |
| No. unique reflections | 54252 | |
| $R_{work}$ / $R_{free}$ | 0.21 / 0.25 | |
| No. atoms | 8697 | |
| Macromolecules | 8575 | |
| Ligands | 63 | |
| Solvent | 132 | |
| *B*-factors | | |
| Wilson | 62.3 | |
| ADP (mean) | | |
| Macromolecules | 82.2 | |
| Ligands | 132.8 | |
| Solvent | 65.9 | |
| R.m.s deviations | | |
| Bond lengths (Å) | 0.007 | |
| Bond angles (°) | 0.898 | |
| **Molprobity** | | |
| All atom clashscore | 13.84 | |
| **Ramachandran** | | |
| Outliers | 0.83% | |
| Allowed | 2.49 % | |
| Favoured | 96.68 % | |

*Values in parentheses are for highest-resolution shell.

**Supplementary Table 3**

**Yeast strains**

| Strain name | Genotype | Notes |
|---|---|---|
| JMM1188 | h- smt0 ade6-704 leu1-32 ura4-D18 | Wild type (WT) |
| JMM1038 | smc6-G551R ade6-704 leu1-32 ura4-D18 | Sergeant *et al.*[1] |
| HQD20 | smc6::loxP-smc6-ura4-loxM ade6-704 leu1-32 ura4-D18 | This study |
| HQD50 | smc6::loxP-smc6-R706C-loxM ade6-704 leu1-32, ura4-D18 | This study |
| HQD87 | smc5::loxP-5'-UTR-smc5-ura4-loxM ade6-704 leu1-32 ura4-D18 | This study |
| HQD90 | smc5::loxP-5'-UTR-smc5-W436A-loxM ade6-704 leu1-32 ura4-D18 | This study |
| HQD92 | smc6::loxP-Smc6-F528A-loxM ade6-704 leu1-32 ura4-D18 | This study |
| HQD98 | smc5::loxP-5'-UTR-smc5-S610G-loxM ade6-704 leu1-32 ura4-D18 | This study |
| HQD99 | smc5::loxP-5'-UTR-smc5-Y612G-loxM ade6-704, leu1-32 ura4-D18 | This study |
| HQD247 | smc5::loxP-smc5-R609E R615E-loxM, ade6-704 leu1-32 ura4-D18 | This study |
| HQD249 | smc5::loxP-smc5-R587E R619E-loxM ade6-704 leu1-32 ura4-D18 | This study |
| YMS83 | smc5+/smc5::loxP-5'-UTR-smc5-ura4-loxM ade6-M210/ade6-M216 leu1-32/leu1-32 ura4-D18ura4-d18 h+/h- smt0 | This study |
| YMS99 | smc5+/smc5::loxP-5'-UTR- smc5-S610G Y612G-loxM ade6-M210/ade6-M216 leu1-32/leu1-32 ura4-D18ura4-d18 h+/h- smt0 | This study |

**Supplementary References**


1. Forster, S., Apostol, L. & Bras, W. Scatter: software for the analysis of nano- and mesoscale small-angle scattering. *Journal of Applied Crystallography* **43**, 639-646 (2010).
2. Durand, D. et al. NADPH oxidase activator p67(phox) behaves in solution as a multidomain protein with semi-flexible linkers. *J Struct Biol* **169**, 45-53 (2010).
3. Petoukhov, M.V. et al. New developments in the ATSAS program package for small-angle scattering data analysis. *Journal of Applied Crystallography* **45**, 342-350 (2012).